Inorg. Chem. **2001,** *40,* 7003−7008

Structure−Spectroscopy Correlation in Distorted Five-Coordinate Cu(II) Complexes: A Case Study with a Set of Closely Related Copper Complexes of Pyridine-2,6-dicarboxamide Ligands

Dana S. Marlin, Marilyn M. Olmstead, and Pradip K. Mascharak*

Department of Chemistry and Biochemistry, University of California, Santa Cruz, California 95064,
and Department of Chemistry, University of California, Davis, California 95616

Received May 18, 2001

Eight Cu(II) complexes with the [Cu(dmppy)] moiety (dmppyH_2 = tridentate ligand *N*,*N*′-dimethylpyridine-2,6-dicarboxamide; H’s are dissociable amide protons) and ligands like pyridine, water, *N*-methylimidazole, substituted and unsubstituted *o*-phenanthroline, and bipyridine have been isolated and structurally characterized. The basal angles of these structurally related five-coordinate Cu(II) complexes (and two previously reported ones) correlate well with the EPR hyperfine splitting parameter $A_{||}$. However, the values of the parameter τ which provides a measure of the degree of square pyramid versus trigonal bipyramid geometry adopted by these complexes do not correlate linearly with the $A_{||}$ values. It is evident that out-of-plane distortions and ligand strain make calculation of τ inconsistent in certain sets of five-coordinate Cu(II) complexes. Structure−spectroscopy correlation involving τ is not feasible in such cases.

Introduction

During the past few decades, a substantial effort has been made to establish correlations between structural and spectral parameters in mono- and multinuclear copper complexes. As a result, structure−spectroscopy correlations for small molecules with four-coordinate Cu(II) centers are relatively abundant in the literature.[1−5] Structural variations in these systems are usually indicated by a tetrahedral distortion index which depends on L−M−L angles and the dihedral angle between the two planes, each of which contain the central Cu atom and two cis ligands.[3] A vast number of Cu(II) complexes have also been isolated that are five- or six-coordinate with long axial bonds due to Jahn−Teller distortion of the d^9 Cu(II) center.[1,6] Structurally, the geometries of the five-coordinate complexes usually range from square pyramidal (SP, C_{4v}) to trigonal bipyramidal (TBP, D_{3h}), with most of the complexes falling between ideal SP and TBP geometry, somewhere along the classical Berry pathway.[6,7] Hathaway and others have put considerable effort into establishing structure−spectroscopy correlations in five-coordinate Cu(II) complexes. The results indicate that significant difficulties arise in such endeavor due to several factors which include, but are not limited to, structural plasticity of the copper complexes and variation in the type of donor ligands within the sets of Cu(II) complexes used.[1,8−11]

In 1984, Addison, Reedijk and co-workers introduced a very useful parameter, τ, which provides a measure of the degree of SP versus TBP geometry adopted by the five-coordinate Cu(II) complexes.[12] This parameter provides a convenient tool for comparing structures of similar five-coordinate Cu(II) complexes.[6−9,13] The parameter τ depends on two angles, α and β. In the distorted square pyramidal geometry shown below, where A is the axial ligand, β is defined as the larger of the basal angles, B−M−C, and α is the remaining angle between D−M−E. The parameter τ is then defined as $(\beta - \alpha)/60$, and its value varies from 0 (in SP) to 1 (in TBP) and is often reported as a percent value (% $\tau = \{(\beta - \alpha)/60\}100$).

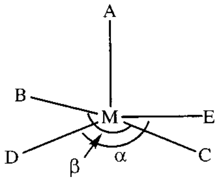

Following the introduction of the parameter τ, several groups have attempted to correlate τ with the EPR hyperfine coupling constant $A_{||}$ of five-coordinate Cu(II) complexes. The large hyperfine splitting constant $A_{||}$ is usually well resolved and easily measured and therefore provides a convenient spectroscopic

---

* To whom correspondence should be addressed at the University of California at Santa Cruz.

(1) Hathaway, B. J. Copper. In *Comprehensive Coordination Chemistry*; Pergamon Press: Oxford, U.K., 1987; Vol. 5, pp 533−774 and references therein.

(2) Peisach, J.; Blumberg, W. E. *Arch. Biochem. Biophys*. **1974**, *165*, 691.

(3) Addison, A. W. Spectroscopic and redox trends from model copper complexes. In *Cooper Coordination Chemistry: Biochemical and Inorganic Perspectives*; Karlin, K. D., Zubieta, J., Eds.; Adenine Press: New York, 1983.

(4) Solomon, E. I.; Baldwin, M. J.; Lowery, M. D. *Chem. Rev*. **1992**, *92*, 521.

(5) Knoblauch, S.; Benedix, R.; Ecke, M.; Gelbrich, T.; Sieler, J.; Somoza, F.; Hennig, H. *Eur. J. Inorg. Chem*. **1999**, 1393.

(6) Addison, A. W.; Rao, T. N.; Reedijk, J.; van Rijn, J.; Verschoor, G. C. *J. Chem. Soc., Dalton Trans*. **1984**, 1349.

(7) Addison, A. W.; Rao, T. N.; Sinn, E. *Inorg. Chem*. **1984**, *23*, 1957.

(8) Murphy, G.; O’Sullivan, C.; Murphy, B.; Hathaway, B. *Inorg. Chem*. **1998**, *37*, 240.

(9) O’Sullivan, C.; Murphy, G.; Murphy, B.; Hathaway, B. J. *J. Chem. Soc., Dalton Trans*. **1999**, 1835.

(10) Berry, S. *J. Chem. Phys*. **1960**, *32*, 933.

(11) Muetterties, E. L.; Guggenberger, L. J. *J. Am. Chem. Soc*. **1974**, *96*, 1748.

(12) Addison, A.; Rao, T.; Reedijk, J.; van Rijn, J.; Verschoor, G. *J. Chem. Soc., Dalton Trans*. **1984**, 1349.

(13) Manikandan, P.; Thomas, J. K. R.; Manoharan, P. T. *J. Chem. Soc., Dalton Trans*. **2000**, 2779.

10.1021/ic010523n CCC: $20.00

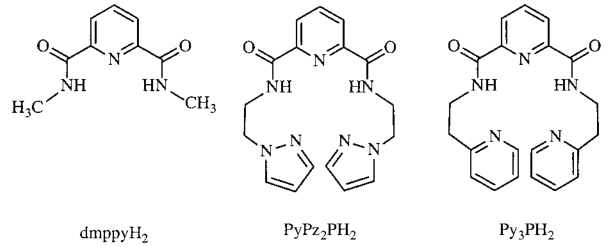

$dmppyH_2$ $PyPz_2PH_2$ Py_3PH_2

Figure 1.

handle for structure−spectroscopy correlation.[4,14,15] Since the hyperfine splitting is sensitive to the degree of orbital overlap between the magnetic (e_g) orbital of the Cu(II) center and the donor atoms around it, it is sensitive to the type of ligand coordinating to the Cu(II) center.[16] Accurate correlation between τ and $A_{||}$ however requires precise estimate of τ in a series of similar Cu(II) complexes with varying structural parameters.

Over the past few years, we[17−21] and others[22−24] have recognized the strong donor capacity of the pyridine-2,6-dicarboxamide moiety in transition metal complexes. In the present study, we have synthesized a series of five-coordinate Cu(II) complexes with the tridentate ligand *N*,*N*′-dimethylpyridine-2,6-dicarboxamide ($dmppyH_2$, where H's represent dissociable amide protons) in which the rigid and almost planar pyridine-2,6-dicarboxamido unit binds copper in the *mer* fashion while the remaining two coordination positions are occupied by ligands that alter the metric parameters in a systematic manner. The complexes are abbreviated and numbered as follows: $[Cu(dmppy)(py)]_2$ (**1**); $[Cu(dmppy)($*N*-MeIm$)]_2$ (**1a**); $[Cu(dmppy)(H_2O)(py)]$ (**2**); [Cu(dmppy)(DMF)(py)] (**2a**); [Cu(dmppy)(bpy)] (**3**); $[Cu(dmppy)(Me_2\text{-}bpy)]$ (**4**); [Cu(dmppy)(*o*-phen)] (**5**); $[Cu(dmppy)(Me_2\text{-}phen)$ (**6**).[25] The Cu(II) complexes of the ligands *N*,*N*′-bis[2-(1-pyrazolyl)ethyl]pyridine-2,6-dicarboxamide ($PyPz_2PH_2$) and *N*,*N*′-bis(2-(2-pyridyl)ethyl)-pyridine-2,6-dicarboxamide (Py_3PH_2), namely $[Cu(PyPz_2P)]$ (**7**)[17] and $[Cu(Py_3P)]$ (**8**),[18] respectively, are also included (Figure 1). With this set of Cu(II) complexes in hand, we have analyzed the effects of small structural variations on the hyperfine splitting parameter $A_{||}$ values. In such attempt, we have encountered a problem relating to distortion due to ligand strain and its effects on the calculation of τ. Since steric constraints from multidentate ligands often results in displacement of the Cu(II) center from either or both planes defined by BAC and DAE, consistent measurements of β and α are not straightforward.[14,15] In such systems, if the difference between α and β is small, then slight structural variation within a similar set of complexes may introduce ambiguity; i.e., what is defined as α in one complex could be defined as β in the next and visa versa. This problem has not been a serious one in some previous works most possibly due to the lack of sufficient number of systematically distorted complexes required to address this issue.[15] Our analysis of the $\tau-A_{||}$ correlations show that (a) changes in the individual basal angles within the present set of complexes correlate well with $A_{||}$ values and (b) significant out-of-plane distortion of the Cu(II) ion in five-coordinate complexes may lead to a situation where calculation of τ by conventional means becomes inconsistent.

Experimental Section

Materials. *N*,*N*′-Dimethyl-2,6-pyridinedicarboxamide ($dmppyH_2$) was prepared according to a literature procedure.[26] The preparation of $[Cu(py)_4](ClO_4)_2$ and $[Cu(DMF)_6](ClO_4)_2$ and their utility as good starting materials will be reported in a separate paper.[27] The complexes $[Cu(PyPz_2P)]$ (**7**) and $[Cu(Py_3P)]$ (**8**) were prepared according to published procedures.[17,18] Sodium hydride (NaH), pyridine, *N*-methylimidazole, bipyridine, 6,6′-dimethyl-2,2′-dipyridyl, 1,10-phenanthroline, and 2,9-dimethyl-1,10-phenanthroline were purchased from Aldrich Chemical Co. and used without further purification. Pyridine was distilled from BaO while *N*-MeIm was distilled from sodium prior to use. Acetonitrile (CH_3CN), dimethylformamide (DMF), tetrahydrofuran (THF), and toluene were obtained from Fischer Chemical Co. and distilled from CaH_2 and BaO (for CH_3CN and DMF, respectively) and sodium/benzophenone (for THF and toluene) prior to use.

Preparation of Compounds. $[Cu(dmppy)(py)]_2$ (1). To a solution of 0.23 g (1.2 mmol) of $dmppyH_2$ in 15 mL of THF was added a batch of 0.057 g (2.4 mmol) of NaH, and the mixture was allowed to stir for 1 h. Next, a solution of 0.70 g of $[Cu(py)_4](ClO_4)_2$ (1.2 mmol) in 40 mL of CH_3CN was added to it and the mixture was stirred overnight. The volume of the reaction mixture was reduced to 20 mL under vacuum, and the mauve precipitate of **1** was filtered off (yield: 80%). Selected IR frequencies (KBr disk, cm^{-1}): 2913 (w), 2860 (w), 1630 (s), 1599 (s), 1579 (s), 1451 (m), 1382 (m), 1298 (m), 1075 (m), 842 (w), 761 (m), 712 (m), 684 (m), 572 (m).

$[Cu(dmppy)($*N*-MeIm$)]_2$ (1a). A batch of 0.032 g (1.3 mmol) of NaH was added to a solution of 0.13 g (0.66 mmol) of $dmppyH_2$ in 10 mL of DMF, and the mixture was stirred until a clear orange solution was obtained. To this was then added a solution of 0.46 g (0.66 mmol) of $[Cu(DMF)_6](ClO_4)_2$ in 5 mL of DMF followed by 0.54 g (6.6 mmol) of *N*-MeIm. The mixture was stirred for 1 h, and then DMF was distilled off under vacuum. The purple residue was washed with two 15 mL portions of CH_3CN and dried in vacuo (yield: 0.23 g, 52%). Selected IR frequencies (KBr disk, cm^{-1}): 3128 (w), 1600 (s), 1579 (s), 1545 (w), 1406 (m), 1392 (m), 1376 (w), 1302 (w), 1147 (m), 1108 (s), 844 (w), 764 (w), 684 (w), 624 (m), 575 (w).

$[Cu(dmppy)(py)(H_2O)]$ (2) and [Cu(dmppy)(py)(DMF)] (2a). A batch of 0.10 g (0.15 mmol) of complex **1** was disolved in 2 mL of DMF, and the solution was stored at room temperature in a capped vial. Dark blue crystals of **2a** (0.01 g, 27% yield) were collected from this solution after 48 h. The filtrate from this reaction was then mixed with 1 mL of diethyl ether, and the mixture was allowed to stand at room temperature for 3 days. The few blue blocks of **2** (yield ∼ 10%) formed during this time were collected by filtration. Selected IR frequencies (KBr disk, cm^{-1}) for **2a**: 2912 (w), 2861 (w), 1690 (m), 1603 (s), 1569 (s), 1438 (w), 1388 (s), 1372 (s), 1303 (s), 1075 (w), 1028 (w), 834 (w), 740 (m), 688 (m), 680 (m), 589 (w). Electronic absorption spectrum in DMF of **2a** [λ_{max}, nm (ϵ, $M^{-1}\cdot cm^{-1}$)]: 590 (175).

[Cu(dmppy)(bpy)] (3). To a solution of 0.11 g (0.60 mmol) of $dmppyH_2$ in 10 mL of DMF was added a batch of 0.03 g (1.2 mmol) of NaH and the mixture stirred until a clear orange colored solution

---

(14) Hoskins, B. F.; Whillans, F. D. *Coord. Chem. Rev.* **1972**, *9*, 365.

(15) Arriortua, M. I.; Mesa, J. L.; Rojo, T.; Debaerdemaeker, T.; Beltrán-Porter, D.; Stratemeier, H.; Reinen, D. *Inorg. Chem.* **1988**, *27*, 2976.

(16) Weil, J. A.; Bolton, J. R.; Wertz, J. E. *Electron Paramagnetic Resonance*; *Elementary Theory and Practical Applications*; Wiley-Interscience: New York, 1994.

(17) Chavez, F. A.; Olmstead, M. M.; Mascharak, P. K. *Inorg. Chim. Acta* **1998**, 269.

(18) Chavez, F. A.; Olmstead, M. M.; Mascharak, P. K. *Inorg. Chem.* **1996**, *35*, 1410.

(19) Chavez, F. A.; Rowland, J. M.; Olmstead, M. M.; Mascharak, P. K. *J. Am. Chem. Soc.* **1998**, *120*, 9015.

(20) Marlin, D. S.; Mascharak, P. K. *Chem. Soc. Rev.* **2000**, *29*, 69.

(21) Rowland, J. M.; Thornton, M. L.; Olmstead, M. M.; Mascharak, P. K. *Inorg. Chem.* **2001**, *40*, 1069 and references therein.

(22) Patra, A. K.; Ray, M.; Mukherjee, R. *Polyhedron* **2000**, *19*, 1423.

(23) Patra, A. K.; Mukherjee, R. *Inorg. Chem.* **1999**, *38*, 1388.

(24) Ray, M.; Ghosh, D.; Shirin, Z.; Mukherjee, R. *Inorg. Chem.* **1997**, *36*, 3568.

(25) The abbreviations are as follows. pyridine (py); *N*-methylimidazole (*N*-MeIm); bipyridine (bpy); 6,6′-dimethyl-2,2′-dipyridyl (Me_2-bpy); 1,10-phenanthroline (*o*-phen); 2,9-dimethyl-1,10-phenanthroline (Me_2-phen).

(26) Marlin, D. S.; Olmstead, M. M.; Mascharak, P. K. *J. Mol. Struct.* **2000**, *554*, 211.

(27) Marlin, D. S.; Olmstead, M. M.; Mascharak, P. K. Manuscript in preparation.

Table 1. Summary of Crystal and Intensity Collection Data and Structure Refinement Parameters for $[Cu(dmppy)(py)]_2$ (**1**), $[Cu(dmppy)(py)(H_2O)]$ (**2**), [Cu(dmppy)(bpy)] (**3**), $[Cu(dmppy)(Me_2\text{-}bpy)]\cdot NaClO_4\cdot CH_3CN$ (**4**$\cdot NaClO_4\cdot CH_3CN$), $[Cu(dmppy)(o\text{-}phen)]\cdot NaClO_4\cdot 1.5CH_3CN$ (**5**$\cdot NaClO_4\cdot 1.5CH_3CN$), and $[Cu(dmppy)(Me_2\text{-}phen)]\cdot NaClO_4\cdot 1.2CH_3CN\cdot 0.4tol$ (**6**$\cdot NaClO_4\cdot 1.2CH_3CN\cdot 0.4tol$)

params	**1**	**2**	**3**	**4**$\cdot NaClO_4\cdot CH_3CN$	**5**$\cdot NaClO_4\cdot 1.5CH_3CN$	**6**$\cdot NaClO_4\cdot 1.2CH_3CN\cdot 0.4tol$
empirical formula	$C_{28}H_{28}Cu_2N_8O_4$	$C_{14}H_{16}CuN_4O_3$	$C_{19}H_{17}CuN_5O_2$	$C_{23}H_{24}ClCuN_6NaO_6$	$C_{24}H_{15.5}ClCuN_{6.5}NaO_6$	$C_{28.2}H_{27.8}ClCuN_{6.2}NaO_6$
M_r	667.66	351.85	410.92	602.46	612.91	671.55
cryst color, habit	red needle	blue plate	blue plate	blue plate	teal blue plate	blue plate
T, K	138(2)	90(2)	90(2)	130(2)	130(2)	92(2)
cryst system	monoclinic	monoclinic	orthorhombic	monoclinic	monoclinic	monoclinic
space group	$P2_1/n$	$P2_1/c$	Pbca	$P2_1/c$	$P2_1/n$	$P2_1/c$
a, Å	9.1734(10)	8.6463(6)	8.9912(3)	12.925(4)	11.546(2)	15.780(2)
b, Å	12.4461(19)	10.5912(8)	15.3143(5)	15.762(5)	10.741(2)	15.334(2)
c, Å	12.2131(14)	16.5888(12)	25.3592(9)	14.171(5)	21.402(3)	13.898(2)
α, deg	90	90	90	90	90	90
β, deg	96.866(9)	95.5090(10)	90	107.21(3)	96.201(15)	110.912(7)
γ, deg	90	90	90	90	90	90
V, Å^3	1384.4(3)	1512.10(19)	3491.8(2)	2757.7(16)	2638.4(8)	3141.4(7)
Z	2	4	8	2	4	4
d_{calcd}, g cm^{-1}	1.602	1.546	1.563	1.451	1.543	1.420
abs coeff, μ, mm^{-1}	2.322	1.462	1.277	0.952	0.998	0.844
GOF[a] on F^2	1.079	1.046	1.078	1.023	1.028	1.065
R_1,[b] %	3.39	2.44	3.34	7.54	6.99	7.08
R_{w2},[c] %	9.26	6.99	7.72	17.93	16.8	19.15

[a] $GOF = [\Sigma[w(F_o^2 - F_c^2)^2](M - N)]^{1/2}$ (M = number of reflections, N = number of parameters refined). [b] $R_1 = \Sigma||F_o - F_c||/\Sigma|F_o|$. [c] $R_{w2} = [\Sigma[w(F_o^2 - F_c^2)^2]/\Sigma[w(F_o^2)^2]]^{1/2}$.

was obtained. A solution of 0.42 g (0.60 mmol) of $[Cu(DMF)_6](ClO_4)_2$ in 5 mL of DMF was then added to it followed by 0.094 g (0.6 mmol) of bpy. Upon continued stirring, complex **3** precipitated out of this solution as a crystalline blue solid, which was filtered off after 8 h (yield: 0.18 g, 73%). Selected IR frequencies (KBr disk, cm^{-1}): 2951 (w), 1625 (s), 1597 (s), 1578 (s), 1478 (w), 1444 (m), 1380 (m), 1296 (m), 1068 (m), 838 (w), 766 (m), 744 (m), 684 (w). Electronic absorption spectrum in DMF [λ_{max}, nm (ϵ, $M^{-1}\cdot cm^{-1}$)]: 580 (110).

$[Cu(dmppy)(Me_2\text{-}bpy)]\cdot NaClO_4\cdot CH_3CN$ (4$\cdot NaClO_4\cdot CH_3CN$). A solution of 0.05 g (0.27 mmol) of Me_2-bpy in 1 mL of CH_3CN was added to a solution of 0.10 g (0.15 mmol) of **1** and $NaClO_4$ (0.019 g) in 1 mL of CH_3CN, and the mixture was allowed to stir for 1 h. The resultant blue solution was then filtered, and diethyl ether was allowed to slowly diffuse into the filtrate. Large blue blocks of **4**$\cdot NaClO_4\cdot CH_3CN$ were collected within 24 h (yield: 0.07 g, 80%). Selected IR frequencies (KBr disk, cm^{-1}): 2863 (w), 1597 (s), 1576 (s), 1466 (m), 1392 (m), 1375 (m), 1302 (m), 1110 (s), 1073 (s), 800 (m), 760 (w), 687 (w), 624 (m), 597 (w). Electronic absorption spectrum in DMF [λ_{max}, nm (ϵ, $M^{-1}\cdot cm^{-1}$)]: 585 (130).

$[Cu(dmppy)(o\text{-}phen)]\cdot NaClO_4\cdot 1.5CH_3CN$ (5$\cdot NaClO_4\cdot 1.5CH_3CN$). A solution of 0.06 g (0.3 mmol) of *o*-phen monohydrate in 1 mL of CH_3CN was added to a solution of 0.10 g (0.15 mmol) of **1** and $NaClO_4$ (0.019 g) in 1 mL of CH_3CN, and the mixture was allowed to stir for 1 h. The resultant blue solution was then filtered, and the filtrate was stored in a vial with a 2 mL portion of toluene layered on it. Large blue prisms of **5**$\cdot NaClO_4\cdot 1.5CH_3CN$ were collected after 48 h (yield: 0.08 g, 85%). Selected IR frequencies (KBr disk, cm^{-1}): 1576 (s), 1516 (m), 1428 (m), 1395 (m), 1303 (m), 1146 (s), 1110 (s), 1089 (s), 849 (m), 762 (w), 730 (m), 684 (w), 637 (m), 627 (m). Electronic absorption spectrum in DMF [λ_{max}, nm (ϵ, $M^{-1}\cdot cm^{-1}$)]: 580 (135).

$[Cu(dmppy)(Me_2\text{-}phen)]\cdot NaClO_4\cdot 1.2CH_3CN\cdot 0.4tol$ (6$\cdot NaClO_4\cdot 1.2CH_3CN\cdot 0.4tol$). This complex was synthesized by the same procedure that afforded **5**. The only difference was that Me_2-phen was used instead of *o*-phen. Large blue prisms of **6**$\cdot NaClO_4\cdot 1.2CH_3CN\cdot 0.4tol$ (tol = toluene) were collected within 48 h in 65% yield. Selected IR frequencies (KBr disk, cm^{-1}): 2914 (w), 2862 (w), 1622 (s), 1596 (s), 1576 (s), 1501 (m) 1430 (w), 1395 (s), 1376 (m), 1302 (m), 1108 (s), 1072 (s), 867 (m), 841 (m), 761 (m), 731 (w), 687 (w), 623 (m), 574 (w), 551 (w). Electronic absorption spectrum in DMF [λ_{max}, nm (ϵ, $M^{-1}\cdot cm^{-1}$)]: 580 (125).

X-ray Data Collection and Structure Solution and Refinement. Red needles of **1** suitable for X-ray analysis were obtained upon cooling a solution of **1** in CH_3CN/pyridine (~10:1 v/v) to −20 °C over a 48 h period. Blue plates of **2** were obtained from a solution of **1** in DMF/ether (~5:1 v/v) which was stored at room temperature for a period of 4 days. Large blue plates of **3** were grown from a saturated solution of **3** in DMF. Complex **4** cocrystallized with $NaClO_4$ into large blue plates when diethyl ether was allowed to diffuse into a solution of **4** and 1 equiv of $NaClO_4$ in CH_3CN. Complexes **5** and **6** also required $NaClO_4$ for crystallization and crystals of these two complexes contained $NaClO_4$ in them. For both these complexes, toluene was layered on their solutions in CH_3CN with 1 equiv of $NaClO_4$. Such attempts afforded large blue plates of **5** and **6** which were suitable for X-ray analysis. Diffraction data for **1** were collected at 138 K on a Siemens P4 diffractometer while data for complexes **2**, **3**, and **6** were collected at 90 K on a Bruker SMART 1000 system. For complexes **4** and **5**, data were collected at 130 K on a Siemens P3 instrument. Mo Kα (0.710 73 Å) radiation was used in all cases, and the data were corrected for absorption. Intensities of two standard reflections showed only random fluctuations of less than 1% during the course of data collection. The structures were solved using the standard SHELXS-97 package.

Machine parameters, crystal data, and data collection parameters for **1**−**3**, **4**$\cdot NaClO_4\cdot CH_3CN$, **5**$\cdot NaClO_4\cdot 1.5CH_3CN$, and **6**$\cdot NaClO_4\cdot 1.2CH_3CN\cdot 0.4tol$ are summarized in Table 1 while selected bond distances and angles are listed in Table 2. Complete crystallographic data for these complexes have been submitted as Supporting Information.

Other Physical Measurements. A Perkin-Elmer 1600 FTIR spectrophotometer was employed to monitor the infrared spectra. Absorption spectra were recorded on a Perkin-Elmer Lambda 9 spectrophotometer. The EPR spectra at X-band frequencies were obtained with a Bruker ESP-300 spectrometer.

Results and Discussion

The new starting material $[Cu(py)_4](ClO_4)_2$ allows a convenient and straightforward method for synthesizing the dimeric complex $[Cu(dmppy)(py)]_2$ (**1**) from weakly coordinating solvents such as CH_3CN and THF. In turn, complex **1** undergoes facile substitution reactions to generate the monomeric complexes $[Cu(dmppy)(H_2O)(py)]$ (**2**), [Cu(dmppy)(DMF)(py)] (**2a**), $[Cu(dmppy)(Me_2\text{-}bpy)]$ (**4**), [Cu(dmppy)(*o*-phen)] (**5**), and $[Cu(dmppy)(Me_2\text{-}phen)]$ (**6**). Complex **3** is readily formed in the reaction of $[Cu(DMF)_6](ClO_4)_2$ with $dmppy^{2-}$ and bpy in DMF and crystallizes out from the reaction mixture in high yield within minutes. Complexes **4**−**6** are particularly sensitive to moisture and hence require very dry conditions for their isolation. Also, if one does not isolate these complexes quickly

Table 2. Selected Bond Distances (Å) and Bond Angles (deg) for Complexes **1**−**8** (Using the Atom Labels Defined in Figure 5a), Along with Parameters ρ (Å),[a] σ (Å),[b] τ (%),[c] θ (deg),[d] T^5,[e] $g_{\parallel}$, and $A_{\parallel}$ (G) for the Relevant Complexes

	1	**2**	**3**	**4**	**5**	**6**	**7**	**8**
Cu−N_{p1}	2.008(2)	2.0204(9)	2.0012(13)	1.996(4)	2.001(5)	2.008(4)	1.979(2)	1.985(2)
Cu−N_{py}	1.923(2)	1.9268(9)	1.9330(13)	1.930(4)	1.925(4)	1.929(4)	1.928(2)	1.942(2)
Cu−N_{p2}	1.989(2)	2.0101(10)	2.0096(13)	1.998(4)	1.992(5)	2.013(4)	2.002(2)	2.003(2)
Cu−A_L	2.807(2)[f]	2.3107(9)	2.2237(14)	2.189(5)	2.239(4)	2.224(4)	2.260(3)	2.172(2)
Cu−N_L	1.982(2)	1.9891(9)	2.0461(13)	2.041(4)	2.041(4)	2.016(4)	2.024(2)	2.089(2)
A_L−Cu−N_L		95.58(3)	76.46(5)	77.81(17)	78.17(17)	78.78(16)	101.32(9)	101.15(9)
A_L−Cu−N_{py}		94.96(3)	121.14(5)	128.41(18)	101.91(17)	118.91(14)	111.01(10)	119.62(9)
A_L−Cu−N_{p1}		96.72(3)	91.46(5)	99.77(18)	93.30(18)	100.93(15)	102.96(10)	102.06(9)
A_L−Cu−N_{p2}		93.72(3)	99.37(5)	95.72(18)	102.11(18)	94.08(14)	84.93(9)	87.40(9)
N_{py}−Cu−N_{p1}	80.03(10)	80.23(4)	80.14(5)	79.54(17)	80.09(19)	80.30(16)	80.11(10)	79.68(10)
N_{py}−Cu−N_{p2}	80.56(10)	80.12(4)	79.99(5)	80.06(18)	79.66(19)	79.17(15)	80.67(10)	79.96(10)
N_L−Cu−N_{p1}	101.73(10)	97.83(4)	102.14(5)	95.72(18)	101.62(1 9)	97.47(17)	92.88(10)	91.21(9)
N_L−Cu−N_{p2}	98.56(10)	99.86(4)	96.61(5)	99.77(18)	98.58(19)	100.31(16)	102.87(10)	104.76(9)
N_{py}−Cu−N_L	173.98(10)	169.44(4)	162.35(5)	153.78(1 9)	178.24(1 9)	162.31(1 7)	147.66(10)	139.21(9)
N_{p1}−Cu−N_{p2}	158.37(10)	158.45(4)	160.12(5)	159.28(1 8)	156.7(2)	158.65(1 6)	160.75(9)	159.63(10)
ρ	0.199	0.187	0.014	0.077	0.242	0.124	0.021	0.015
σ	0.110	0.302	0.265	0.211	0.268	0.235	0.283	0.278
τ		18	4	9		6	22	34
θ		1.5	5.4	2.7		4.1	9.7	9.2
T^5		0.86	0.90	0.91		0.90	0.88	0.92
$g_{\parallel}$		2.21	2.20	2.20	2.20	2.20	2.20	2.20
$A_{\parallel}$		191	180	174	182	180	161	154

[a] Cu distance from the N_{p1}−N_{py}−N_{p2} plane. [b] Cu distance from the N_{p1}−A_L−N_{p2} plane. [c] $\tau = \{(\beta - \alpha/60)\}100$. [d] Deviation from 90° of the angle between the planes defined by N_{p1}−N_{py}−N_{p2} and A_L−Cu−N_L. [e] Ratio of average in-plane Cu−N distances versus Cu−A_L distance. [f] Distance for Cu1−O2A.

from the reaction mixtures, the blue solutions turn brown indicating decomposition. We have discovered that the addition of $NaClO_4$ allows rapid crystallization of **4**−**6** and hence provides a convenient way to isolate these species in high yield. We have also prepared the dimeric complex $[Cu(dmppy)(N\text{-}MeIm)]_2$ (**1a**) (Figure S1, Supporting Information) from $[Cu(DMF)_6](ClO_4)_2$ and *N*-MeIm in DMF. This complex can be isolated in good yield and may also be used as a precursor for the preparation of other complexes containing the [Cu(dmppy)] unit.

In the solid state, the structures of **1** and **1a** comprise dimeric units resulting from interactions between the carbonyl oxygen on the $dmppy^{2-}$ ligand frame of one [Cu(dmppy)] unit to the Cu center of another (Figure 2a, Cu−O = 3.34 Å).[28] It is interesting to note that the red crystals **1** and **1a** are isolated from blue solutions. Despite the presence of a large excess of py or 1-MeIm, respectively, in such reaction mixtures, in no case were we able to isolate momoneric species with these relatively strong donors bound at the axial sites. The situation is somewhat different when the reaction mixtures have traces of water. The monomeric species $[Cu(dmppy)(H_2O)(py)]$ (**2**) can be isolated as a minor product under such conditions. However, attempts to synthesize **2** with a stoichiometric equivalent of water invariably fail and the starting blue solutions change to brown and afford unidentifiable products. In **2**, the water molecule is weakly coordinated at the axial site (Cu−O = 2.31 Å, Table 2) and is stabilized by an extensive network of hydrogen bonding (Figure S2, Supporting Information). Spectroscopic data indicate that [Cu(dmppy)(DMF)(py)] (**2a**) also contains a molecule of DMF (O-bonded) at the axial site. We have used the structural data of **2** for the "solvent bound" species in our structure−spectroscopy correlation since determination of the structure of **2a** was hindered due to twinning in the crystal lattice.

In the structures of **3**−**6**, the $dmppy^{2-}$ ligand and the bidentate ligand (bpy, Me_2-bpy, *o*-phen, Me_2-phen, respectively) coordinate to the Cu(II) center in a [3 + 2] fashion. The values of the dihedral angle (θ) between the two ligand planes are listed in Table 2. Interestingly, the crystal packing in the structure of **5** differs from that in **3**, **4**, and **6** due to the presence of π-stacking of two [Cu(dmppy)] moieties in the unit cell (Figure 2b). The

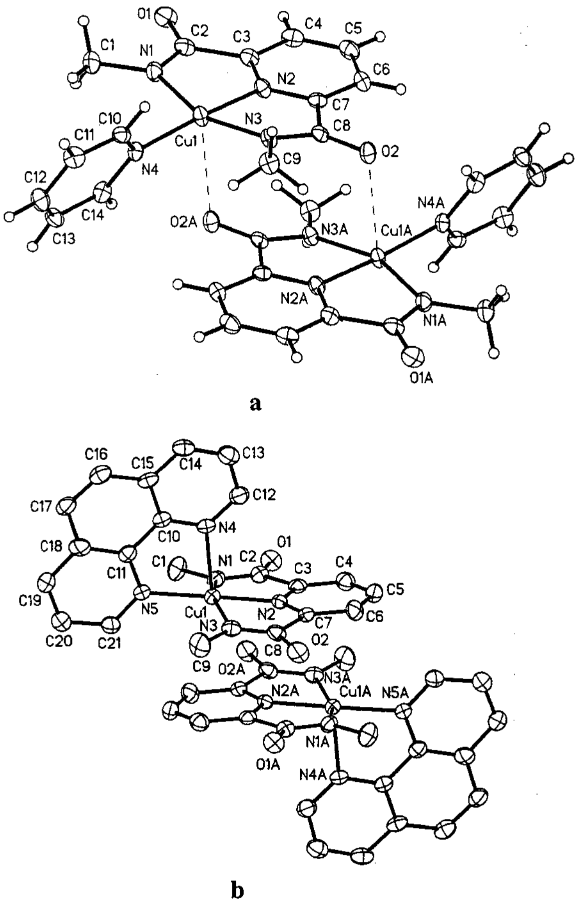

Figure 2. Thermal ellipsoid (probability level 50%) plot of (a) $[Cu(dmppy)(py)]_2$ (**1**) and (b) [Cu(dmppy)(*o*-phen)] (**5**) showing the numbering scheme. In the case of **5**, H atoms, $NaClO_4$, and the lattice solvent molecules are omitted for the sake of clarity.

---

(28) The structure of **1a** is shown in Figure S1.

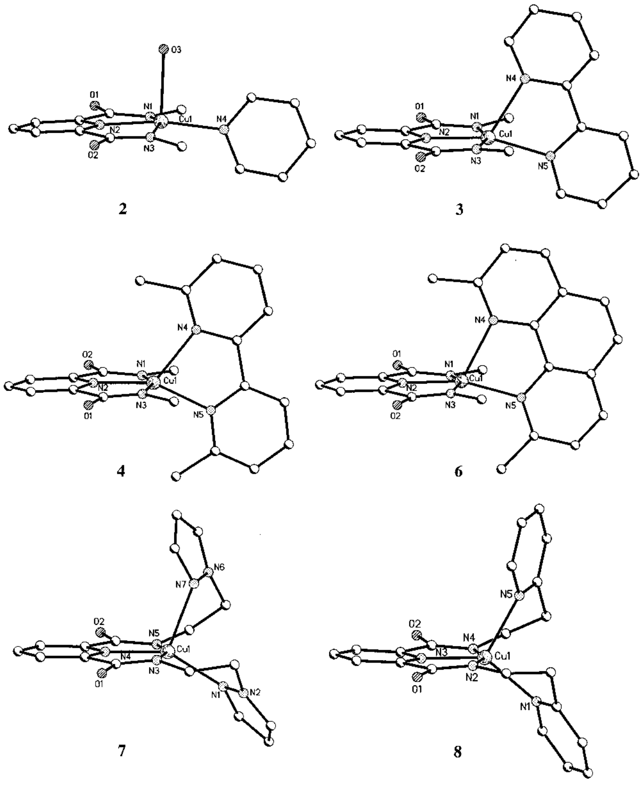

Figure 3. Perspective views of complexes **2**−**4** and **6**−**8** looking along the N_{amido}−Cu−N_{amido} axis. The numbering schemes for **2**−**4** and **6** are similar while those for **7** and **8** are as reported in refs 17 and 18.

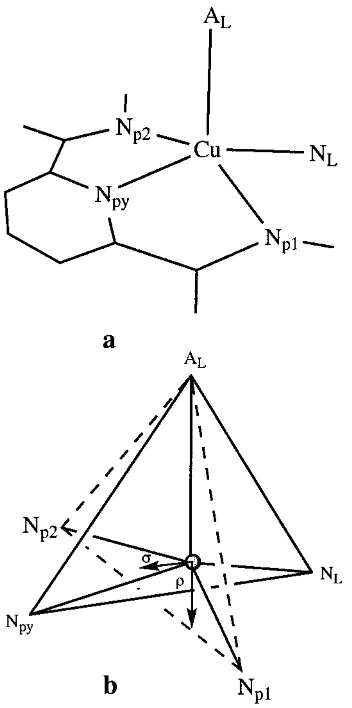

Figure 4. (a) Structural frame for the Cu(II) complexes along with the general labeling scheme used for listing data in Table 2 and (b) the out-of-plane distortion of the Cu(II) ion from the $N_{p1}N_{py}N_{p2}$ plane, ρ, and the distance of Cu(II) from the $N_{p1}A_LN_{p2}$ plane, σ.

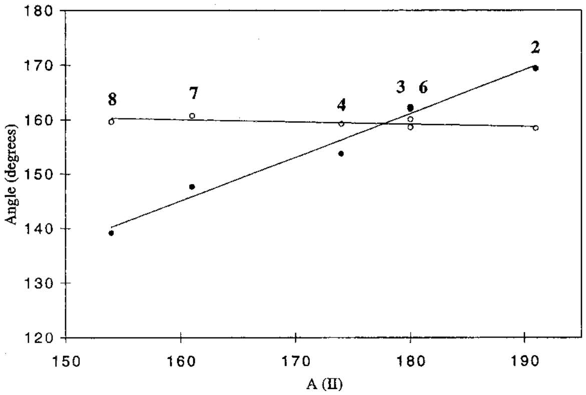

Figure 5. Plot of the two basal angles N_{py}−Cu−N_L and N_{p1}−Cu−N_{p2} vs the $A_{\|}$ values for complexes **2**−**4** and **6**−**8**.

π interaction between adjacent [Cu(dmppy)] units causes the *o*-phen ligands of the two neighboring complexes to move out of the [Cu(dmppy)] plane resulting in an unusually high N_{py}−Cu−N_L angle (178.24°, Table 2). Such distortion in the solid-state structure prohibits inclusion of the structural parameters of **5** in any structure−spectroscopy correlation.

The pyridine-2,6-dicarboxamido unit of the dmppy^{2-} ligand (Figure 1) is a strong chelator. This is reflected in the short Cu−N_{py} and Cu−N_{amido} bond distances (average N_{py} = 1.93 Å, average N_{amido} = 2.00 Å, Table 2) noted in complexes **1**−**8**. The N_{amido}−N_{py}−N_{amido} portion changes very little from complex to complex. Perspective views of complexes **2**−**4** and **6**−**8** as one looks at them along the N_{amido}−Cu−N_{amido} axis are shown in Figure 3. This figure provides a clear idea of the major changes in the geometries of these complexes as a result of variation in the remaining two sites.

The X-band EPR spectra of all the Cu(II) complexes have been run in DMF/toluene (70:30 v/v) glass at 100 K. The spectra are typical of monomeric Cu(II) with $d_{x^2-y^2}$ ground state.[1,16] In all cases, the clean spectra (Figure S3, Supporting Information) allow easy and accurate determination of the $A_{\|}$ values which are included in Table 2.

Figure 4 illustrates the structural frame for the Cu(II) complexes along with the labeling scheme used for listing data in Table 2 and in our subsequent structure−spectroscopy correlation. In this drawing, N_{py}, N_{p1}, and N_{p2} respectively represent the pyridine nitrogen and the two carboxamido nitrogens of the pyridine-2,6-dicarboxamido moiety. The axial ligand, A_L is defined by the longest Cu−ligand bond in the complex (∼2.2−2.3 Å, Table 2) and N_L represents the remaining fifth ligand. The out-of-plane distortion of the Cu(II) ion from the $N_{p1}N_{py}N_{p2}$ plane is ρ while σ is the distance of Cu(II) from the $N_{p1}A_LN_{p2}$ plane (Figure 4b). The values of ρ and σ are also listed in Table 2. By convention, the parameter τ is calculated from τ (%) = $\{(\beta - \alpha)/60\}100$, where the angle β is defined as the larger of the two basal angles. In ideal SP geometry β = 180°, α = 180°, and τ = 0%, while in ideal TBP geometry, β = 180°, α = 120°, and τ = 100%.

In Figure 5, we have plotted the two basal angles N_{py}−Cu−N_L and N_{p1}−Cu−N_{p2} versus the $A_{\|}$ values for **2**−**8** (with the exception of **5**) following identification of the axial ligand (A_L) by the longest Cu−ligand distance. In this plot, the solid and open circles represent the N_{py}−Cu−N_L and N_{p1}−Cu−N_{p2} angles, respectively. It is evident from Figure 5 that the basal angles themselves correlate very well with the $A_{\|}$ values. However, the plots in Figure 5 also reveal a problem. As a result of the large out-of-plane distortions of the Cu(II) center (ρ and σ in these complexes), the larger angle (β) in some cases is between N_{p1}−Cu−N_{p2} (in **4**, **7**, and **8**) and in others (**2**, **3**, and **6**) it is between N_{py}−Cu−N_L. The axes that define α or β thus switch from one complex to another in this set. A consequence of this switch becomes apparent when we take the larger of the two angles N_{p1}−Cu−N_{p2} or N_{py}−Cu−N_L (Table 2) as β, calculate τ values, and plot them against $A_{\|}$. The plot, shown in Figure

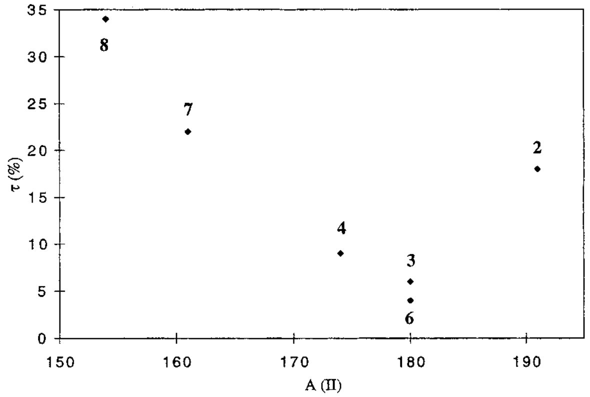

Figure 6. Plot of τ vs $A_{\|}$ values for **2**−**4** and **6**−**8**.

6, exhibits a point of inflection where the angles α and β crossover. This plot clearly indicates that a linear correlation between τ and $A_{\|}$ values exists in the set **4**, **7**, and **8** where α and β have been defined consistently. Similar correlation exists for **2**, **3**, and **6**. However, the linear correlation between τ and $A_{\|}$ values breaks down if we take the whole set of complexes under consideration. The α and β crossover appears to be responsible for this break down. The results therefore suggest that (a) when structural features such as out-of-plane distortions and ligand strain make α and β values comparable and (b) when β values are especially low (~160°), calculation of τ becomes inconsistent and structure−spectroscopy correlation involving τ is not feasible any more.

The negative slope in the plot of τ vs the hyperfine coupling constant $A_{\|}$ for complexes **8**, **7**, **4**, and **3** (or **6**) makes intuitive sense when one considers overlap of orbitals in the equatorial plane of these complexes. The magnetic orbitals for SP and TBP geometry are $d_{x^2-y^2}$ and d_{z^2}, respectively, and the axes along which these orbitals lie for the [Cu(dmppy)] unit are shown in Figure 7. As the SP character of the complexes decreases (τ increases) in the order **8** > **7** > **4** > **3** (or **6**), the overlap between the magnetic orbital ($d_{x^2-y^2}$) and the ligand orbital is reduced and this translates into a decrease in $A_{\|}$ values. Similar behavior has been observed in other sets of Cu(II) complexes.[29,30]

Conclusion

Since its introduction to the chemistry of copper, τ values of Cu(II) complexes have been correlated with spectral and electrochemical parameters. However, in many cases, the complexes under consideration include different ligands[6,29] and hence effect(s) of minor structural variations on τ values, particularly the effect of systematic small distortions, has not been studied in detail. We have illustrated here that, for structurally similar five-coordinate Cu(II) complexes, one must use caution while defining angles for the calculation of τ values. Distortions in ligand frame could result in situations where such definition becomes inconsistent and leads to breakdown of correlation between spectral parameters and τ values. We plan to pursue similar studies to establish this fact in a few series of Cu(II) complexes with different sets of ligands.

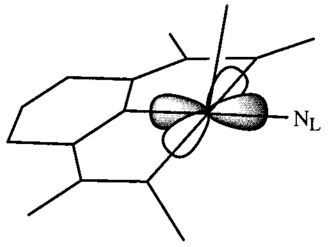

SP

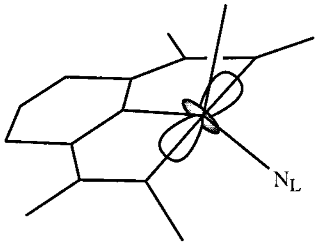

TBP

Figure 7. Magnetic orbitals for SP and TBP geometry.

Acknowledgment. This research was supported by a grant from the National Science Foundation (CHE-9818492). The Bruker SMART 1000 diffractometer was funded in part by the NSF Instrumentation Grant CHE-9808259. The experimental assistance of Rebecca Helms is gratefully acknowledged.

Supporting Information Available: A perspective view of [Cu(dmppy)(N-MeIm)]$_2$ (**1a**) (Figure S1), a view of [Cu(dmppy)(py)(H$_2$O)] (**2**) showing H-bonding (Figure S2), X-band EPR spectra (DMF/toluene glass, 100 K) of **2a**, **4**, and **8** (Figure S3), tables of X-ray data for **1**−**8**, and X-ray crystallographic files, in CIF format, for the structure determination of **1**−**8**. This material is available free of charge via the Internet at http://pubs.acs.org.

IC010523N

---

(29) Addison, A. W.; Burke, P. J.; Henrick, K.; Rao, T. N.; Sinn, E. *Inorg. Chem.* **1983**, *22*, 3645.

(30) Miyoshi, K.; Tanaka, H.; Kimura, E.; Tsuboyama, S.; Murata, S.; Shimizu, H.; Ishizu, K. *Inorg. Chim. Acta* **1983**, *78*, 23.